Identification, modeling and observation of disturbing effects in EUV interferometer lithography

Mohammed Saïb, Maxime Besacier, Christophe Constancias, Philippe Michallon

Identification, modeling and observation of disturbing effects in EUV interferometer lithography

M. Saïb[*1], M. Besacier[1], C. Constancias[2] and P. Michallon[2]
1. CNRS- LTM Grenoble - MINATEC, 17 rue des Martyrs, 38054 Grenoble, France
2. CEA Grenoble - MINATEC, 17 rue des Martyrs, 38054 Grenoble, France

ABSTRACT

The challenge of the Integrated Circuit size reducing leads to the development of new processes for future years. In the lithography domain, since several years, the EUV Lithography appears as a possible technique to reach the ITRS roadmap requirements. The EUV interferometry Lithography is still nowadays an efficient way to study and improve the EUV resist behaviors. Although the interferometer principle seems to be obvious, the optimization of its use is only reached regarding some huge constraints. In this work accurate numerical models and experimental studies have been developped. It shows that some undesirable effects can reduce the interference region and disturb the contrast of the resist printed lines. The EUV light is identified as the first issue. The beam divergence of EUV light affects the contrast quality of the fringes. The photometry computation, taking into account the optimum angular source light width is then detailed. The second cause is the Fresnel diffraction of light due to boundaries of the grating windows. Its superimposition with diffraction orders induces a damage of local printed interferences. This phenomenon leads to an edge disturbance of the interference fringes. The third cause addressed is the decrease of the interference area by the position of the wafer out of the focal distance. Possible shadowing effects are also shown

Keywords: EUV Lithography, interferometer, diffraction, Fresnel diffraction, modelling, contrast

1. INTRODUCTION

In the microelectronics industry, Moore's Law predicts that the number of transistors in an integrated circuit (IC) doubles every 18 months. This increase leads to a decrease of their dimensions. A continuous improvement of technical and industrial equipments is mandatory to follow this law. The lithography domain, a key step in the manufacturing cycle, is concerned by this trend. The optical transmission lithography shows its physical limits to achieve, in the near future, the dimensions specified. New technologies emerge but are not still well adapted to the industrial production constraints [1,2]. Among the promising technologies, the Extreme UltraViolet (EUV) Lithography is regularly cited [3,4]. Very close to the techniques used up to now, its very short wavelength (13.5 nm) can reach nanoscale dimensions. Nevertheless, many technological barriers must be overcame to meet the requirements. In this context, the parallel development of tools should allow to characterize and analyze the issues. The interferometer appears as a technique to define geometric high resolution with a short exposure time [5-7]. At the EUV wavelength, an Interferometer Lithography (IL) allows characterizing the resists such as their sensitivity [8].
This article addresses, in a global approach, disturbances affecting the quality of the printed interferences. This work starts by the photometry study applied to EUV source. By considering the analytical equation of the contrast of interference fringes, some approaches to ensure a good quality of the resist patterns are proposed. These approaches must take into account the tolerated photons path difference and the optical intensity at the diffraction grating level. In this work, two main optical configurations of the interferometer are considered. For each case, the useful optical intensity is estimated. Then, the impact of the dimensions of diffraction mask on the interferences is shown. Disturbances such as Fresnel diffraction or defocusing are presented and their contribution on the interference damage is shown.

* Mohamed.saib@cea.fr; Phone: +33-438-78-66-07; fax: +33-438-78-58-92

2. PRINCIPLES OF THE INTERFEROMETRY LITHOGRAPHY

The single grating EUV-IL experimental setup is shown in figure 1. It is composed by a light source, ideally generating a collimated beam and with a high average density of radiation. The EUV light is applied to a diffraction grating. The surface of this diffraction mask has two grating windows of width *Cp* and separated by an absorber layer of width *d*. Both windows contain a dense line grating of period *p* to diffract the incident light. The whole grating structure is placed on a silicon membrane of 100nm thickness. The EUV light projected onto the transparent grating windows is diffracted according to several discrete orders. The angles of diffraction orders vary depending on the light wavelength λ and the period of diffraction grating *p*. For a given diffracted order *m*, the diffraction angle θ_m, defined regarding the axis of incidence of light, is written as:

$$\sin\theta_m = m\frac{\lambda}{p} \tag{1}$$

For the 1st order diffraction, the intersection of the +1st order with the -1st order from both different gratings is responsible for the appearance of a stationary sine wave. It prints in the photoresist, a dense line grating with a period two times lower than the grating period. Since the intersection of the +1st and -1st diffracted orders occurs with an angle $2.\theta_m$, the width of the recombination area varies with the distance between the grating mask and the resist (figure 1). The maximum width of this area is obtained for the focal distance:

$$W_D = \frac{\left(\frac{Cp+d}{2}\right)}{\tan\left(\arcsin\left(\frac{\lambda}{p}\right)\right)} \tag{2}$$

We introduce the Depth of Focus (*DoF*) as the distance between the nearest and farthest plane compared to the focal plane (W_D) for which interference fringes are printed. This is expressed:

$$DoF = \frac{Cp}{\tan\left(\arcsin\left(\frac{\lambda}{p}\right)\right)} \tag{3}$$

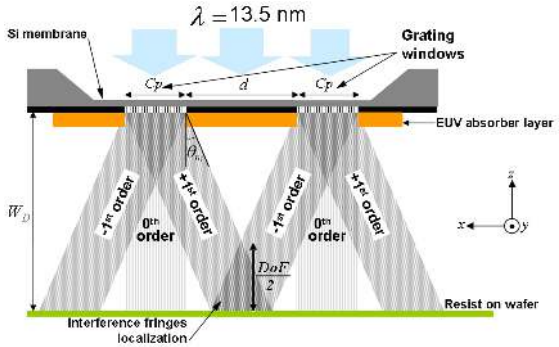

Figure 1. Interference lithography principle using a single grating mask. The grating surface is composed by two grating windows (*Cp* width), separated by a distance *d*. The +1st order and -1st order interfere and generate fringes with half grating pitch.

3. OPTICAL CONFIGURATION OF THE INTERFEROMETER

Considering an EUV beam generated by an extended source (figure 2), the circular radiation source surface with a radius *s* generates a divergent beam characterized by its half-divergence angle θ_s. This light beam is diffracted by the grating mask and the recombination fo the +/-1 diffraction orders gives interference fringes. The resulting intensity according to the *x*-axis is written as:

$$I(x) = 2\cdot I_0\left(1 + C\cdot\cos\frac{4\pi x}{p}\right) \tag{4}$$

where x is the position of the optical intensity on the resist plane and C is the contrast of interferences fringes linked to the properties of the light beam. It is expressed as:

$$C = \sin c\left(\frac{\pi \cdot (d + Cp) \cdot 2 \cdot \delta\theta}{\lambda}\right) \tag{5}$$

where sinc is the sinus cardinal, $\delta\theta$ is the half angular width of the source observed from the grating plane. It is written as:

$$tg(\delta\theta) = \frac{s}{D} \tag{6}$$

s is the radius of the source and D the distance between the source and the grating mask plane as shown in figure 2. An arbitrary minimum value of contrast established at 63% guaranteed good quality of printed interference fringes on the resist. By putting this value in equation 5, we define the maximum source angular width admitted:

$$\delta\theta \leq \frac{\lambda}{4 \cdot (d + Cp)} \tag{7}$$

Two possible configurations are considered in following subsections to respect the condition of the equation 7.

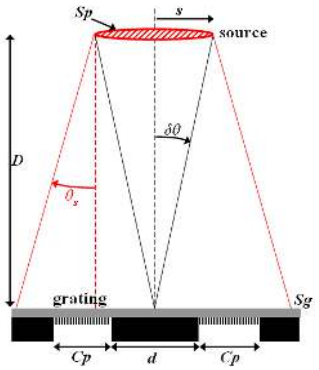

Figure 2. Schematic representation of source of diameter s and surface Sp positioned at distance D from interferometer grating mask. The source is defined by it angular width $\delta\theta$, and delivers a beam characterized by it half angle divergence θ_s.

3.1. Distance EUV source – diffraction grating

The first approach is to improve the partial collimation of the beam by the setting of the distance between the EUV source and the diffraction grating. If the source is far enough to the grating, the beam rays are considered nearly parallel. It means if the distance D is $D = \frac{s}{tg(\delta\theta)}$. On the other hand, the EUV source must provide enough energy at the desired wavelength to carry out prints in a reasonable time. The optical intensity per grating window surface is written:

$$I_1 = \frac{F \cdot Sw}{Sg^2} = \frac{F \cdot Cp \cdot L}{\left(\pi(D \cdot tg\theta_s + s)^2\right)^2} \tag{8}$$

where F is the flux of the EUV source, Sw the surface of each grating window, Sg the surface of the EUV beam at the level of the grating plane, D the distance between the source and the diffraction grating, and L the length of the grating window.

The following example gives some numerical values: Considering a diffraction grating with $d = Cp$ = 30µm, and length L=800µm, irradiated with light wavelength 13.5nm by an EUV source with a radius of 400µm. This source delivers a photon flux 10^{16} ph/s at the level of its output. It has a half divergence angle of 5.58mrad. These dimensions leads to a half angular width $\delta\theta \leq 56.3$µrad as expressed in the equation 7. It also induces a distance D = 704cm. For this distance D, the optical intensity I_1 is 9.8 10^8 ph/(s·Sw). Note that the distance of the source at 704cm from the diffraction grating is relatively difficult to implement for experiments.

3.2. The diaphragm insertion

In the second optical configuration, the improvement of the partial light collimation is made by the cancellation of photons which not ensure the condition described by the equation 7. This is done by spatially filtering the light source. It consists of a diaphragm insertion with a radius R on the EUV beam (figure 3). The radius of the diaphragm is determined depending on the distance D_2:

$$R = D_2 \cdot tg(\delta\theta) \tag{9}$$

This distance D_2 must be as low as possible to have the maximum intensity on gratings. In order to reduce the photon loss, the diaphragm is placed at the source exit. Since the y-axis does not require any filtering, the orders recombination does not occur in this direction, the circular diaphragm can be replaced by a rectangular slit of width $2R$ and length L equal to the length of transparent windows grating.

In this case, the optical intensity per grating window surface is written:

$$I_2 = \frac{F \cdot L^2 \cdot Cp \cdot D_2 \cdot tg(\delta\theta)}{\pi \cdot s^2 \cdot (D_2 \cdot tg(\theta_s) + D_2 \cdot tg(\delta\theta))(L + 2 \cdot D_2 \cdot tg(\theta_s))} \tag{10}$$

The numerical application with the same configuration described in 3.1 and with the slit position at a distance D_2 = 20cm (arbitrarily chosen) shows that the slit shape will be rectangular with a width 22µm and a length (L) 800µm. The EUV source provides in this case an optical intensity I_2 equal to $1.27 \cdot 10^{12}$ ph/(s·*Sw)*.

The numerical applications for both configurations show that using a slit in the interferometer set-up is interesting since it allows putting the source at a reasonable distance of the diffraction grating (20cm instead 704cm) while keeping the collimation of the source beam. The intensity I_2 is then is higher than I_1.

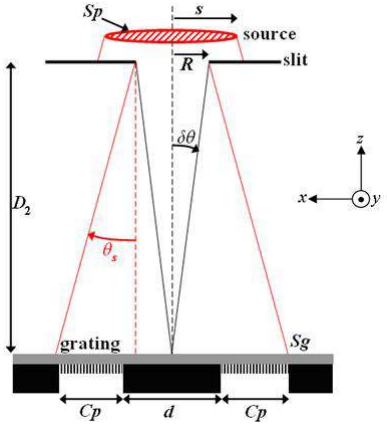

Figure 3. Schematic representation of a source spatially filtered by a slit insertion of width $2R$ and at a distance D_2 from grating mask.

4. EXPERIMENTAL RESULTS

In this section, experimental results of prints made at the EUV wavelength are shown and compared with modeling results. The undesirable effects on the prints induced by the diffraction mask are addressed. They are divided into three disturbances. First, the Fresnel diffraction effect which affects the profile of the interferences fringes area printed in resist. The second effect, which reduces the interference area width, is linked to the position of the resist plane out the focal plane. The third effect called shadowing effect causes also the decrease of the interference area by absorption of diffracted orders near the edges of gratings windows Note that this last effect is easy to avoid, regarding some constraints on experimental process. The print tests have been carried out thanks to the EUV synchrotron source Aladdin from SRC (Synchrotron Radiation Center) of Wisconsin [9]. In the experimental tool, the diffraction grating is put on a 3 moving axis stand to address multiple resist prints. The exposure time (close to 1second) is tuned for each experimental configuration to insure a good print quality. The diffraction mask is built on a silicon membrane and has four different couples of gratings with periods of 200nm, 140nm, 100nm and 80nm [10]. The focal distance W_D remains the same for the four grating and is equal to 600µm. It means that the distance d is different and adjusted for each couple of gratings. The width of windows Cp is 50µm for 200nm and 100nm gratings and 60µm for 140nm and 80nm gratings. The total length L of gratings is 800µm. This experimental system is put within a vacuum vessel and is mechanically stabilised.

4.1. The Fresnel diffraction effect

The first effect addressed is the Fresnel Diffraction [11]. The effect is a boundary effect and it appears when the light passes through the grating transparent windows. This phenomenon is resulted by a non uniform and localized variation of the transmitted optical intensity. This overlapping with the fringes, in the interference area, induces a damage of local interferences shape especially if the Fresnel intensity shows some significant variations (figure 4). The profile of this intensity can be determined regarding the following parameters: the wavelength, the distance between the grating and the resist and the width of the transparent window. In the diffraction theory, the Fresnel number gives a numerical definition of this profile with the following expression.

$$N_F = \frac{Cp^2}{4 \cdot \lambda \cdot W_{\exp}} \tag{11}$$

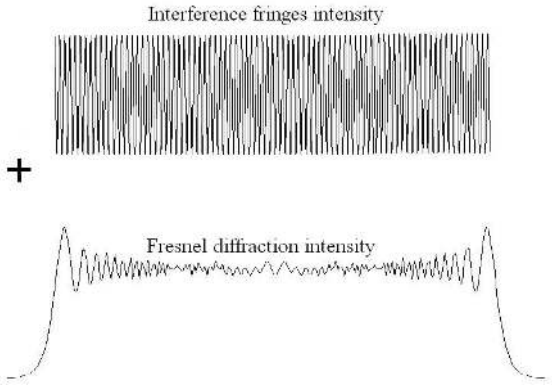

Figure 4. Schematic representation of optical intensities delivered to the resist for printing. Two intensities are shown: The interference fringes intensity which has a period of an half of the mask grating period and the Fresnel intensity which has a variable period of 4µm near boundaries. Note that this scheme does not respect the period scale.

4 examples of diffracted intensities computed for an EUV light are shown in figure 5. The comparison of these four figures shows the intensity profile evolution versus the Fresnel number. The case N_F =0,75 corresponds to the most important distance W_{exp}. A strong intensity variation is then observed in the area of the diffraction window. The intensity ratio between center and border values is close to 350%. The W_{exp} decrease leads to a N_F increase (figure 5b). In this case the intensity profile remains inhomogeneous on the width Cp. 3 undulations are observed. For N_F =9 (figure 5c), the intensity window is larger and the mean value is steady. It remains, nevertheless some important local undulations. Finally for a high N_F =25 (figure 5d), the intensity shows undulations with a weak magnitude, especially for the center area ,far from the boundaries of grating. The contrast of one undulation is defined by the following relationship:

$$C = \frac{I_{\max} - I_{\min}}{I_{\max} + I_{\min}} \tag{12}$$

With $I_{\max}$ and $I_{\min}$ the extremum intensity values of the same undulation.
For instance, on the figure 5d, the contrasts of the five first undulations from the border to the center are respectively 28%, 16%, 13%, 10% and 9%. For N_F > 25, the Fresnel diffraction curves keep the same profile than N_F = 25, then it influence on the interference fringes remains the same.

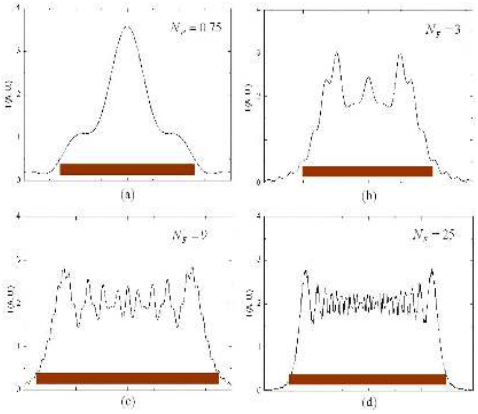

Figure 5. Fresnel diffraction intensity shape for: (a) N_F=0.75, (b) N_F=3, (c) N_F=9 and (d) N_F=25. The brown rectangle represents the diffraction window width.

The Fresnel effect is superimposed to all diffracted orders. In the interference area, the Fresnel effect causes a disturbance of the profile of the dense lines profile printed in resist. The best way to only observe this effect is on the 0th order, it means without any other effects such as interferences fringes. The figure 6a shows a MEB picture of the printed resist at the 0th order. In this case the distance between diffraction grating and the resist plane is 560um. Printed patterns are observed within the rectangle of the diffraction window. The diameter of these patterns decreases when going to the exposed surface center. Beyond the nineth pattern, disturbances printed in the resist vanish and the surface becomes homogeneous. The nineth undulation is considered as the last undulation of disturbance. The contrast of this undulation is 7%.

The Fresnel effect is also modeled as shown in figure 6b thanks to the computation of the Fresnel integrals leading to the diffracted intensity. The picture shows the aerial image of the diffracted intensity at resist level. Computations have been made with the same dimensional configuration as the experiments, it means for a rectangular diffracted window (60µm x 800µm) at a distance of 560um to the resist plan. N_F values are then not the same regarding the axis x or y. N_{Fx} = 119 and N_{Fy} = 21160. The diameter of the largest circle is 2.5um. This value matches well with the experimental measurement.

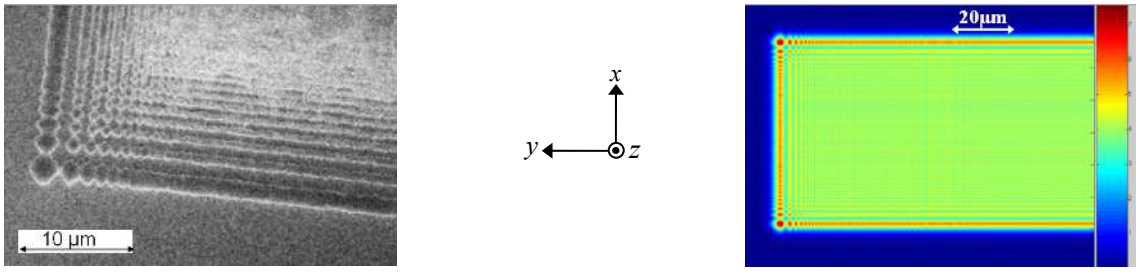

(a) (b)

Figure 6. a) SEM image of resist patterned under 0th order diffracted by the grating window of 800µm in length and 60µm in width. The exposure is performed at work distance W_{ext}=560µm. b) 2D modelling of the aerial image of the diffracted intensity with 0th order. This computation is performed for the same structural and experimental dimensions with Fig. 6a.

The figure 7 shows a modeling case for a Fresnel number N_F < 3 leading to a strong inhomogeneous diffracted intensity on 0^{th} order. To obtain this picture, the dimensions configuration is the following:

Cp = 5um

L = 800um

W_{exp} = 2mm

The N_F is 0,23 in the x axis and 5925 in the y axis. Intensity values on boundaries (in blue color) are five times lower than those in center (in red color). The resulting contrast is close to 60%, strongly higher than the 7% acceptable. This configuration causes a degradation of the fringe contrast in the middle of the interference area. This configuration has not

been experimentally implemented but it shows that a low Fresnel number on an axis is not available for a diffraction mask design. In order to avoid this kind of situations, the following condition is applied on the diffraction window width: $N_F = \frac{Cp^2}{4 \cdot \lambda \cdot W_{\exp}} < 25$ allows the limitation of these disturbances. The diffraction window width must then check the relation:

$$Cp \geq 10\sqrt{\lambda \cdot W_{\exp}} \tag{13}$$

For an interferometer at 13.5nm and a diffraction grating with a working distance at 600µm, the width *Cp* must be larger than 29µm.

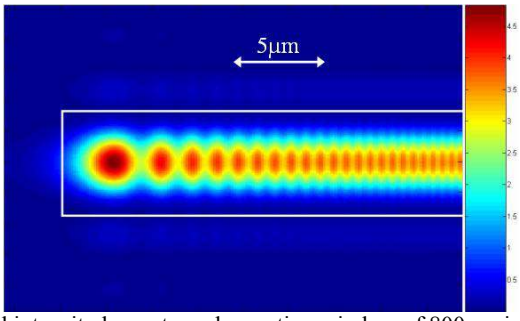

Figure 7. 2D modelling of the diffracted intensity by rectangular grating window of 800µm in length, 5µm in width and focal plane at 2mm. White rectangle outlines the limits of the diffraction window.

4.2. The Focus effect

The diffraction mask causes a second disturbance which is the decrease of the interferences area. Regarding the principle of the interferometer (figure 1), the interferences appear on an area width *Cp* which is the width of the diffraction gratings if the focal distance is respected. However, the experiments show that the interferences area can be reduced if the experimental distance between the gratings and the resist plan is different to the focal distance (600µm). The figure 8 shows a global view of the interferences area printed in the resist by a grating with a width *Cp* = 60µm and a working distance W_{exp} = 560µm. Three different areas can be distinguished. A grey central area contains the printed periodic lines with a period of 70nm and along the *y*-axis. On top and bottom sides of this central area, two other darkest areas are observed with a width $2x_p$ (figure 9). There is no print within. Indeed, since the resist is out of the focal distance, there is a decrease of the interference area of x_p on each side compared with the optimal width at the distance focal. This decrease is expressed by the equation 14:

$$x_p = \left|W_{\exp} - W_D\right| \cdot tg\left(\arcsin\left(\frac{\lambda}{p}\right)\right) \tag{14}$$

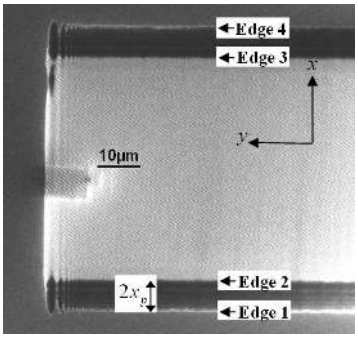

Figure 8. Overview image of the interference region printed in the resist using a grating period of 140nm. Interferometric fringes are localized in the central region (bright) of rectangle. Dark regions on top and bottom side of image appear because of the gap between the focal distance (600µm) and the experimental work distance (560µm).

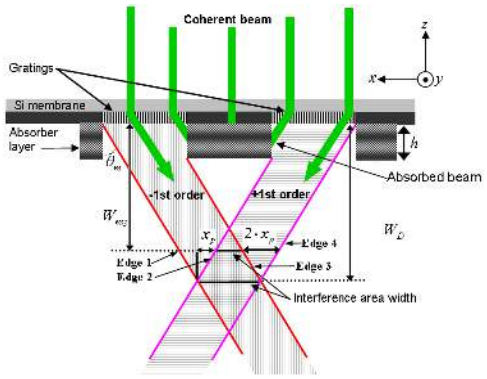

Figure 9. Schematic illustration of single grating interferometer. Coherent light is diffracted into -1st and +1st orders and give a maximum interference width at focal distance. For work distance out of the focal plane, the width decrease gradually. The 1st order diffracted near tot the edge of grating windows is absorbed by absorber layer (shadowing effect).

Since there is only one order in these both areas (+1 or -1) no interferences fringes can be observed and the absence of these dark areas on lateral sides of the picture shows that it is directly dependent on the direction of the diffraction orders. For the experiment leading to the figure 8, the grating period is 140nm and the working distance is 560µm whereas the focal distance is 600µm. It leads to a width decrease of 7,6µm of the interference print area (3,8µm on each side). The width decreases from 60µm to 52,4µm.

In spite of the straight shape of the boundaries of the diffraction windows, the dark areas on top and bottom sides shows some disturbances at edges 1, 2, 3 and 4 (figure 8) along the *y* axis and look like Fresnel diffraction previously observed on *z* axis (see section 4.1). The diffraction on the first order is oblique regarding the *z* axis and exists only in the *xoz* plan (there is no diffraction in the *yoz* plan). +1 and -1 orders of diffraction have also Fresnel diffraction phenomenon on their propagation axis (figure 10). The projection of these Fresnel diffraction effects in the resist plan shows an inverse shape of Fresnel figures on edge 1 and edge 2 and on edge 3 and edge 4, mainly because that edges 1 and 3 are provided by the -1 diffraction order of the left grating while edges 2 and 4 are provided by the +1 order of the right grating.

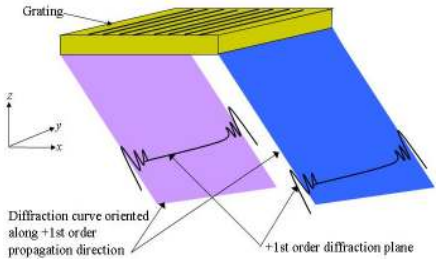

Figure 10. Schematic representation of +1st order light diffracted by a grating. The Fresnel diffraction effect is superimposed to the 1st order and it component according x-axis is printed.

4.3. The Shadowing effect

Another effect which leads to disturbances on the interference area is dependent on the position and on the height of the absorber layer between both diffraction gratings (figure 9). The incident light comes to gratings with a normal incidence to the grating plan. Close to boundaries of the diffraction window, the diffracted light ray runs up against the absorber layer. For a given absorber layer with a height *h*, the decrease of the width of the interference area on each side is:

$$x_n = h \cdot \tan\left(\arcsin\left(\frac{\lambda}{p}\right)\right) \qquad (15)$$

The total width decrease due to shadowing effect is then $2x_n$. Considering the order of magnitude of the height *h*, this effect on the width decrease remains low compared with the working distance effect (focalisation effect). For a grating with a 140nm period and an absorber height of 0,4µm, the resulting decrease is 0.048µm. It shows that this effect is less disturbing compared to the defocus effect. Moreover, this effect can be cancelled by a flip of the absorber pattern (face to the light source and not face to the resist anymore). It must be considered for the experimental exposures.

5. CONCLUSIONS

A fully detailed study of disturbances affecting interference fringes obtained thanks to an EUV interferometer is presented. It is based on an experimental campaign on an EUV synchrotron source and on the modeling of phenomena occuring in this kind of structures during the interference print process. Considering the contrast and the size of the interference area as key parameters, disturbance causes can be clearly identified and their impacts are estimated:
The EUV beam divergence effect leading to a contrast damage is reduced thanks to put a slit in front of the light source allowing a spatial filtering and only keeping EUV photons available for a good resist print quality.

- The Fresnel effect generated by the grating diffraction leads to a decrease of interference contrast on interference area boundaries for a Fresnel number $N_F < 25$.
- The defocusing of the resist plan on the diffraction grating plan leading to a decrease of the width of the interference area.
- The oblique incidence of the +1 and -1 diffracted orders leads to a disturbance of the boundaries of the interference area.

Acknowledgment: The authors would like to acknowledge J. Wallace of the center for nanotechnology of Wisconsin-Madison University through experimental collaboration at the synchrotron radiation center.

REFERENCES

[1] W. Chen and H. Ahmed, Appl. Phys. Lett. 62 (13), 1499(1993)
[2] S. Y. Chou, P. R. Krauss, W. Zhang, L. Guo, and L. Zhuang, J. Vac. Sci. Technol. B15(6), 2897 (1997).
[3] B. Wu and A. Kumar, J. Vac. Sci. Technol. B 25(6), 1743 (2007).
[4] C. W. Gwyn, R. Stulen, D. Sweeney, and D. Attwood, J. Vac. Sci. Technol. B 16(6), 3142(1998).
[5] H. H. Solak, D. He, W. Li, and F. Cerrina, J. Vac. Sci. Technol. B 17(6), 3052(1999).
[6] H. H. Solak, J. Micro/Nanolith. MEMS MOEMS 8(2), 021204 (2009).
[7] R. Gronheid and M. J. Leeson, J. Micro/Nanolith. MEMS MOEMS 8(2), 021205 (2009).
[8] W. Hinsberg, F. A. Houle, J. Hoffnagle, M. Sanchez, G. Wallraff, M. Morrison, and S. Frank, J. Vac. Sci. Technol. B 16(6), 3689(1998).
[9] J. Wallace, Y.-C. Cheng, A. Isoyan, Q. Leonard, M. Fisher, M. Green, J. Bisognano, P. Nealey, F. Cerrina, Nuclear Instruments and Methods in Physics Research A 582, 254 (2007).
[10] C. Constancias, B. Dalzotto, and P. Michallon, J. Wallace, M. Saib, J. Vac. Sci. Technol. B 28(1), 194(2010).
[11] M. Born and E. Wolf: Principles of optics (Pergamon Press, Oxford, 1970) 4th ed. P: 421.